Alexandria Engineering Journal (2021) 60, 4663–4675

HOSTED BY

Alexandria University

Alexandria Engineering Journal

www.elsevier.com/locate/aej
www.sciencedirect.com

Bioconvection analysis for Sutterby nanofluid over an axially stretched cylinder with melting heat transfer and variable thermal features: A Marangoni and solutal model

Ying-Qing Song [a], Hassan Waqas [b], Kamel Al-Khaled [c], Umar Farooq [b], Sami Ullah Khan [d], M. Ijaz Khan [e], Yu-Ming Chu [f,g,*], Sumaira Qayyum [h]

[a] College of Science, Hunan City University, Yiyang 413000, PR China
[b] Department of Mathematics, Government College University Faisalabad, 31200, Layyah Campus, Pakistan
[c] Department of Mathematics & Statistics, Jordan University of Science and Technology, P.O. Box 3030, Irbid 22110, Jordan
[d] Department of Mathematics, COMSATS University Islamabad, Sahiwal 57000, Pakistan
[e] Department of Mathematics, Riphah International Universtity, I-14, Islamabad 44000, Pakistan
[f] Department of Mathematics, Huzhou University, Huzhou 313000, PR China
[g] Hunan Provincial Key Laboratory of Mathematical Modeling and Analysis in Engineering, Changsha University of Science & Technology, Changsha 410114, PR China
[h] Department of Mathematics, Quaid-I-Azam University 45320, Islamabad 44000, Pakistan

Received 6 December 2020; revised 7 March 2021; accepted 23 March 2021

KEYWORDS

Sutterby nanofluid;
Bioconvection flow;
Marangoni and solutal boundaries;
Melting phenomenon;
Shooting technique

Abstract This research communicates the thermal assessment of Sutterby nanofluid containing the gyrotactic microorganisms with solutal and Marangoni boundaries. The applications of melting phenomenon and thermal conductivity are also considered. The flow is confined by a stretched cylinder. The prospective of Brownian motion and thermophoresis diffusions are also taken account via Buongiorno nanofluid model. The problem is formulated with help of governing relations and equations which are altered into dimensionless form via appropriate variables. The numerical scheme based on shooting scheme is employed to access the solution. A comparative analysis is performed to verify the approximated solution. The observations reveal that the velocity profile enhanced with the Marangoni number while a declining velocity profile has been observed with Sutterby nanofluid parameter and Darcy resistance parameter. The nanofluid temperature get rise with thermal conductivity parameter and thermal Biot number. An arising profile of nanofluid concentration is observed for concentration conductivity parameter and buoyancy ratio parameter.

* Corresponding author.
E-mail address: chuyuming@zjhu.edu.cn (Y.-M. Chu).

Peer review under responsibility of Faculty of Engineering, Alexandria University.

https://doi.org/10.1016/j.aej.2021.03.056
1110-0168 © 2021 THE AUTHORS. Published by Elsevier BV on behalf of Faculty of Engineering, Alexandria University.

Nomenclature

T	temperature	ε	flow comportment index),
N	microorganisms	C_∞	ambient concentration
T_∞	ambient temperature	K	thermal conductivity
N_∞	ambient microorganisms	D_B	Brownian dissemination
b^2	consistency index	D_T	thermophoresis diffusion coefficient
C_p	specific heat	τ	ratio of operative heat capability
ρ	density	α_1	Sutterby nanofluid parameter
β	curvature parameter	α_2	Darcy resistance parameter
S	sponginess parameter	Nc	bioconvection Rayleigh number
Nr	buoyancy ratio parameter	λ	mixed convection parameter
M	magnetic parameter	Nb	the Brownian motion parameter
Pr	Prandtl number	Le	Lewis number
Nt	thermophoresis parameter	Pe	Peclet number
Lb	bioconvection Lewis number	α	Marangoni number
Me	melting parameter,	A_1	thermal Biot number
Ma	Marangoni ratio parameter	A_3	microorganism Biot number
A_2	concentration Biot number		
C	concentration		

1. Introduction

The term "nanofluid" describes suspended nanoparticles in the standard fluid which are use to enhance the process of mixed heat and mass transfer. The research on nano-materials has drawn the attention of researchers in recent decades due to their significance in bioengineering, electrical appliances, biomaterials, and manufacturing and processing periods. The nano-materials are mixture of solutions of nanometer-sized particles with traditional fluids which was first proposed by Choi [1]. Nano-materials used in this liquid are typically made of metal, carbon steel, and iron oxide, and also carbon nanotubes, and typical fluids take into account water, gasoline and ethylene glycol, etc. The thermal conductivity of nano-materials is greater than that of traditional fluids and consequently, solid materials are used to improve the thermal properties of the base liquids. The presence of solid materials in conventional fluids has now enhanced the characteristics of heat transfer. There are many possible uses of nanofluids for temperature difference, including cooling systems, pharmaceutical procedures, hybrid-powered motors, chillers, temperature reduction, microchips, domestic refrigerators, and fuel cells. They show the growth of thermal conductivity and the coefficient of thermal energy transfer relative to continuous phase fluids. Several scientists and researchers have worked with fluids containing various nano-materials, such as nanostructures, platinum, copper, nitrides, titanium dioxide, carbon graphite, copper oxide, carbides, and silicon dioxide with different base fluids. Buongiorno [2] precisely explored the two irregular slip processes, Brownian motion diffusion, and thermophoresis impact, to increase the convective rate of thermal energy transfer. Islam et al. [3] investigated the motion of the MHD and the heat transfer of the micropolar water nanofluid between the two surfaces of the rotating process. Alempour et al. [4] investigated the effect on the nanofluid flow activity and the heat exchange of the ellipsoid aspect ratio as well as the rotating of the tube wall. Ghalambaz et al. [5] examined the heat transfer pattern in vertical plate with suspension of nanoparticles.

Naga Santoshi et al. [6] carried out a computational model of 3D Casson and Carreau nano-liquids flow through an expansion layer for slip effects. Wang et al. [7] also developed the method of heat exchangers for the creation or degradation of the nanofluid flow Boil heat transfer through the starched surface. Acharya et al. [8] presented a numerical frame work for unsteady stretched flow of nanofluid subject to the non-uniform hear source. In another contribution, Acharya et al. [9] addressed the solar applications of magneto-nanofluid containing the gyrotactic microorganisms. Das et al. [10] inspected the variable thermal aspects of nanofluid configured by a moving wedge in presence of surface slip. Acharya et al. [11] presented a statistical analysis for the multiple slip flow of higher order nanofluid. The radiative transport of nanofluidic confined by a bended surface with additional impact of convective constraints was worked out by Acharya [12]. Tlili et al. [13] test the three-dimensional Powell Eyring flow of nanofluid through the porous channel of Darcy Forchheimer. Amjad et al. [14] inspected the curved surface on which micropolar nano-liquids flow is expelled to observe the work of these flows and the production of heat through a stretched layer. Atashafrooz et al. [15] have studied the effects of the heat transfer rate and Brownian diffusion on the thermal properties of the nanofluid flow toward the inclined step throughout the life of the axial magnetosphere. Mir et al. [16] investigate the results of the Sutterby nano-liquids flow deformed by a linearly stretchable surface. Nawaz et al. [17] explored the effect of hybrid nanoparticles in the thermal efficiency of Sutterby fluids. Bilal et al. [18] investigated the implications of the heat and mass transfer of the Sutterby fluid by assessing the influence of the magnetic field. Hassan et al. [19] presented an experimental analysis regarding the hybrid nanofluid flow. Hosseinzadeh et al. [20] identified the thermal properties of hybrid nano-particles by using MoS_2-TiO_2 nanoparticles. In another contribution, Hosseinzadeh et al. [21] accessed the characteristics on hybrid nanofluid subject to the thermal radiation and octagonal porous medium space. Mahanthesh et al. [22] focused on the wedge flow of hybrid nanofluid.

The process of bioconvection arises based on the average upward migration of microorganisms, which have been denser than the base fluid. The definition of bioconvection refers to the activity of a motile gyrotactic microorganism that says about macroscopic motions. Suspensions of a denser outer surface grow into unstable due to microorganisms collapsing to cause bioconvection. There are two groups of microorganisms: reduced organisms and oxytactic organisms. Microorganisms have undoubtedly played an essential role in the advancement of human life, especially because of medical applications. Without the use of microorganisms, life is difficult to lead. These species are too rare to be seen even by an efficient microscope, but they are ideal for the environment. Microorganisms are involved in the processing, production, and environmental mechanisms of bio-fuels, enzymatic biomaterials, mass transport, biotechnology, and biological engineering. Platt [23] first introduced this concept of bioconvection and studied revolving polygonal actions in compact Tetrahymena communities. Plesset and Winet [24] studied the bioconvection of Rayleigh-Taylor instability. Kuznetsov [25] identified the key investigations for the stabilization of nano-materials, namely bioconvection motile microorganisms. Chu et al. [26] investigated the nonlinear thermal radiation and heat-absorbing/generating properties of the nanofluid, such as the motile microorganism, through a bi-directional rotating surface. Islam et al. [27] found an improvement in heat transfer for non-Newtonian nanofluids with motile microorganisms, MHD, and thermal radiation on the stretch sheet. Khan et al.[28] investigated the production of Entropy comprising gyrotactic microorganisms and 2-D steady-state non-Newtonian Oldroyd-B nano-materials employing Cattaneo-Christov heat and mass transfer mechanism over the porous chanel. Waqas et al. [29] measured the process of the bioconvective swimming microorganism in the 2-D constant flow of viscoelastic nano-materials to the vertical surface. Ferdows et al. [30] discussed the concept of nanofluid stability by exponential and increasing cylindrical, comprising of motile gyrotactic microorganisms. Sajid et al. [31] a double-diffuse, hyperbolic nano-liquids tangent analysis involving motile microorganisms and megnetohydrodynaimcs over a stretching sheet. Many investigators are interested in the bioconvection of swimming motile microorganisms as seen in Refs. [32–35]. Aly et al. [36] examined the boundary layer flow for megnetohydrodynaimcs and the power-law nano-liquids composed of gyrotactic motile microorganisms over the exponentially expanded surface, like zero nanoparticles mass flux and convective warming. Rana et al. [37] examined the transverse swimming of nanofluid with the magnetic field and partial slippage, and the significance of Newtonian heating over such a mixed convective heat transfer. Sajid et al. [38] identified the influences of metal nanoparticles, along with bio-convective microbes, on the radiative Reiner-Philippoff fluid due to the stretch sheet. Haq et al. [39] investigated the behavior of mixed convective MHD fluid flow of Eyring-Powell nanofluid causing gyrotactic motile microorganisms in the stretched surface. Shahid et al. [40] investigated the effects of swimming microorganisms on nanofluid MHD with Darcy law through the extension of the surface. Mogharrebi et al. [41] presented a bioconvection of nanofluid based on oxytactic microorganisms confined by rotating cone. Hosseinzadeh et al. [42] analyzed the three-dimensional analysis for cross nanofluid along with motile gyrotactic microorganisms.

The non-Newtonian materials are preferable over viscous fluid in various physiological, industrial and engineering processes due to their multidisciplinary nature. Owing to the well justified fact that the non-Newtonian materials cannot be defined via single relation, therefore distinct constitutive relations are suggested in the literature for incorporating the rheological properties. Among such non-Newtonian materials, the Sutterby fluid is one which successfully represents the high polymer aqueous solutions. This model reflects the viscosity data of variety of polymer melts and polymer solutions. This interesting aspect of this viscous model is it represents the properties of non-Newtonian fluids. This model was originally proposed by Sutterby by investigating the convective heat transfer features from upright *iso*-thermal shell to the Sutterby fluid [43]. Akbar [44] presented the mathematical modeling for Sutterby fluid in stenosed arteries. Hayat et al. [45] discussed the peristaltic flow of Suterby fluid in presence of porous space. Abbas et al. [46] numerical worked out the pulsatile flow of Sutterby fluid in an inclined arterial stenosis.

The Marangoni phenomenon appeared due to the mass transportation of surface tension confined by two fluids interface. This phenomenon is also termed as thermo-capillary convection when it depends upon temperature. James Thomson introduced this phenomenon first time in 1855 [200]. The surrounding fluid particles dragged in a region where the surface tension is relatively higher. The migration of fluid particles from higher surface tension to low surface tension is due to the gradient. The gradient of surface tension is associated with the concentration or temperature gradient. The Marangoni effects captured many practical applications like convection cell, crystal growth, soap films stabilization, Benard cell convection, electron beam melting of metals etc [47–49].

The literature survey presented that a variety of research has been presented deals with the bioconvection flow of nanofluid in presence of various flow features. However, the thermal properties of Sutterby nanofluids containing the gyrotactic microorganisms with Marangoni boundaries have not been presented in the scientific literature. This communication aims to fill this research gap. In order to make the analysis more versatile and interesting, the thermal conductivity and solutal concentration conductivity are assumed as variable. The interesting Brownian and thermophoretic aspects of flow problem are addressed by using Buongiorno nanofluid model. The problem expressed in dimensionless form is numerical tackled with shooting procedure. The present bio-convective thermal nanofluid model conveys many applications in various thermal engineering problems, heating and cooling/cooling systems, bio-medical applications, biomedicine, cancer treatment, manufacturing engineering, bio-fuels, enzymes [50,51].

2. Problem formulation

2.1. Physical consideration:

A two-dimensional flow of Sutterby nanofluid in presence of gyrotactic microorganisms confined by a stretching cylinder has been presented. The applications of Marangoni and solutal boundaries, magnetic force and melting heat transfer are considered. The flow has been assumed to be steady and incompressible. Moreover, the magnetic field is along the r-direction and fluid flow along the z-direction both are perpendicular to each

other. The induced magnetic field and electric field effects are not incorporated under to low magnetic Reynolds number assumptions. The Brownian and thermophoretic prospective of nanofluid are defined by incorporating the Buongiorno model. The Darcy resistance is also taken into account. The flow is induced towards the cylinder having the stretching velocity $U_w(z)$ as shown in Fig. 1. Let T be nanofluid temperature, C be concentration and N reflects the microorganisms density. The nanofluid attained constant surface temperature T_w, concentration C_w and motile density N_w. The variable thermal conductivity and solutal concentration are assumed. The nanofluid temperature, concentration and motile density at free stream are symbolized with T_∞, C_∞ and N_∞, respectively. The velocity component u is assumed along $r-$ direction while velocity component v along $z-$ direction.

2.2. Basic governing equations

In view of the above postulations, the governing equations of the proposed model are [53]:

Conservation of mass:

$$\frac{\partial u}{\partial r}+\frac{u}{r}+\frac{\partial w}{\partial z}=0, \tag{1}$$

Conservation of momentum:

$$u\frac{\partial w}{\partial r}+w\frac{\partial w}{\partial z}=\frac{v^*}{2}\frac{\partial^2 w}{\partial r^2}+\frac{v^*}{2r}\frac{\partial w}{\partial r}-\frac{v^*\varepsilon b^2}{4}\left(\frac{\partial w}{\partial r}\right)^2\frac{\partial^2 w}{\partial r^2}$$

$$-\frac{\sigma B_0^2}{\rho_f}u+\frac{R_z}{\rho_f}+\frac{1}{\rho_f}\begin{bmatrix}(1-C_f)\rho_f\beta^{**}g^*(T-T_\infty)\\-(\rho_p-\rho_f)g^*(C-C_\infty)\\-(N-N_\infty)g^*\gamma(\rho_m-\rho_f)\end{bmatrix}, \tag{2}$$

Conservation of energy:

$$u\frac{\partial T}{\partial r}+w\frac{\partial T}{\partial z}=\frac{1}{\rho c_p}\frac{\partial}{\partial z}\left[k(T)\frac{\partial T}{\partial z}\right]+\frac{K}{(\rho C_p)_f}\left[\frac{\partial^2 T}{\partial r^2}+\frac{1}{r}\frac{\partial T}{\partial r}\right]+\tau\left[D_B\frac{\partial C}{\partial r}\frac{\partial T}{\partial r}+\frac{D_T}{T_\infty}\left(\frac{\partial T}{\partial r}\right)^2\right], \tag{3}$$

For variable thermal conductivity, we use:

$$k(T)=k_\infty\left(1+\in_1\frac{T-T_\infty}{\Delta T}\right) \tag{4}$$

Conservation of concentration:

$$u\frac{\partial C}{\partial r}+w\frac{\partial C}{\partial z}=\frac{1}{\rho c_p}\frac{\partial}{\partial z}\left[D(C)\frac{\partial C}{\partial z}\right]+D_B\left[\frac{\partial^2 C}{\partial r^2}+\frac{1}{r}\frac{\partial C}{\partial r}\right]+\frac{D_T}{T_\infty}\left[\frac{\partial^2 T}{\partial r^2}+\frac{1}{r}\frac{\partial T}{\partial r}\right], \tag{5}$$

For variable concentration relations, let us introduce:

$$D(C)=k_\infty\left(1+\in_2\frac{C-C_\infty}{\Delta C}\right) \tag{6}$$

Conservation of microorganisms:

$$u\frac{\partial N}{\partial r}+w\frac{\partial N}{\partial z}+\left[\frac{\partial}{\partial r}\left(N\frac{\partial C}{\partial r}\right)\right]\frac{bW_c}{(C_w-C_\infty)}=D_m\frac{\partial}{\partial r}\left(\frac{\partial N}{\partial r}\right), \tag{7}$$

The appropriate boundary constraints are [53]:

$$\left.\begin{array}{c} w=U_w(z)=\frac{U_0 z}{l},\ \mu\frac{\partial u}{\partial y}\Big|_{y=0}\frac{\partial\sigma}{\partial x}\Big|_{y=0}=\frac{\partial\sigma}{\partial T}\frac{\partial T}{\partial x}\Big|_{y=0}-\frac{\partial\sigma}{\partial C}\frac{\partial C}{\partial x}\Big|_{y=0},\\ -k\left(\frac{\partial T}{\partial y}\right)\Big|_{y=0}=\rho[\lambda+(T_m-T_0)c_s],-k\frac{\partial T}{\partial y}=h_f(T_w-T),\\ -D_B\frac{\partial C}{\partial y}=h_g(C_w-C),\\ -D_m\frac{\partial N}{\partial y}=h_n(N_w-N),\ at\ r=R\\ w\to 0, C\to C_\infty, T\to T_\infty, N\to N_\infty\ as\ r\to\infty. \end{array}\right\} \tag{8}$$

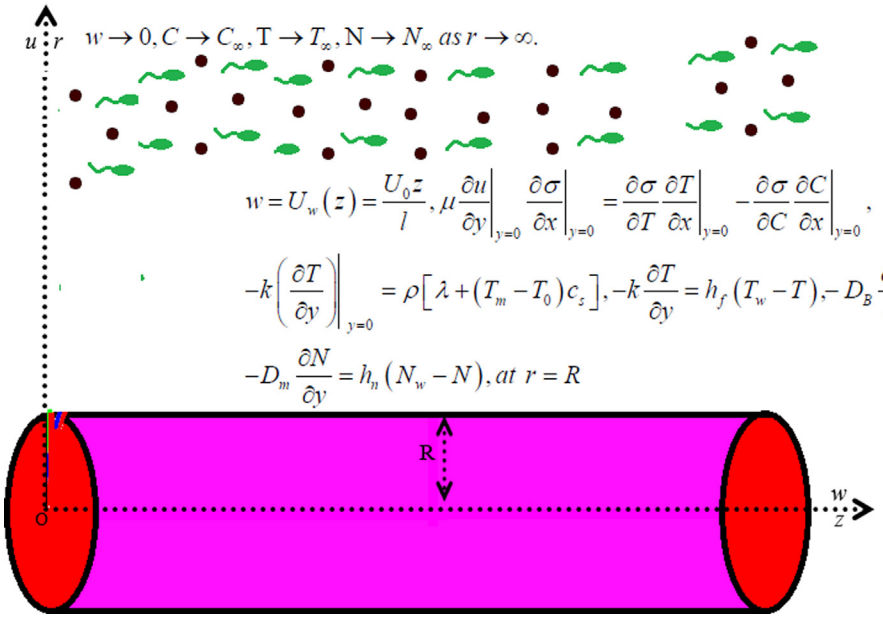

Fig. 1 Physical view of the flow.

The physical variables are ε (flow comportment index), T_∞ (ambient temperature), C_∞ (ambient concentration), N_∞ (ambient microorganisms), k (thermal conductivity), b^2(consistency index), D_B (Brownian dissemination), C_p (specific heat), D_T (thermophoresis diffusion coefficient), ρ (density) and τ (ratio of operative heat capability).

2.3. Similarity transformation

To explain the proposed equations, the following appropriate dimensionless variables are imposed into the basic main equations [53]:

$$\left.\begin{array}{c} u=-\sqrt{\frac{\nu^* U_0}{l}}\frac{R}{r}f(\zeta), w=\frac{U_0 z}{l}f'(\zeta), \zeta=\sqrt{\frac{U_0}{\nu^* l}}\left(\frac{r^2-R^2}{2R}\right), \\ \theta(\zeta)=\frac{T-T_\infty}{T_w-T_\infty}, \phi(\zeta)=\frac{C-C_\infty}{C_w-C_\infty}, \chi(\zeta)=\frac{N-N_\infty}{N_w-N_\infty}. \end{array}\right\}, \tag{9}$$

The dimensionless velocity field, dimensionless temperature field, non-dimensional concentration field and dimensionless microorganism field are f, θ, ϕ and χrespectively.

$$\begin{aligned}(1+2\beta\zeta)f'''+2ff''-2f'^2-\tfrac{\alpha_1}{2}(1+2\beta\zeta)f''^2f'''+\beta f'' \\ -(M+\tfrac{S}{2})f'+\tfrac{1}{12}\alpha_2 f'f''^2 \\ +\lambda(\theta-Nr\phi-Nc\chi)=0,\end{aligned} \tag{10}$$

$$\frac{1}{\mathrm{Pr}}(1+2\beta\zeta)\theta''+(\in_1)\theta''+\in_1\theta'^2-\frac{1}{\mathrm{Pr}}\beta\theta'+f\theta'+(1+2\beta\zeta)[Nb\theta'\phi'+Nt\theta'^2]=0, \tag{11}$$

$$(1+2\beta\zeta)\phi''+(\in_2)\phi''+\in_2\phi^2+\beta\phi'+Le\mathrm{Pr}f\phi'+\frac{Nt}{Nb}[(1+2\beta\zeta)\theta''+\beta\theta']=0, \tag{12}$$

$$(1+2\beta\zeta)\chi''+2\beta\chi'+Lb\chi' f-Pe(\phi''(\chi+\varpi)+\chi'\phi')=0, \tag{13}$$

where $\beta\left(=\frac{1}{R}\sqrt{\frac{\nu^* l}{U_0}}\right)$ is the curvature parameter, $\alpha_1\left(=\frac{\varepsilon b^2 U_0^3 z^2}{l^3\nu^*}\right)$is Sutterby nanofluid parameter, $S\left(=\frac{\nu^* l}{k^* U_0}\right)$is sponginess parameter, $\alpha_2\left(=\frac{\varepsilon b^2 U_0^2 z^2}{l^2 k^*}\right)$is Darcy resistance parameter, $Nr\left(=\frac{(\rho_p-\rho_f)(C_w-C_\infty)}{\rho_f(1-C_\infty)(T_w-T_\infty)\beta^*}\right)$ is buoyancy ratio parameter, $Nc\left(=\frac{\gamma^{**}(\rho_m-\rho_f)(N_w-N_\infty)}{\rho_f(1-C_\infty)\left(T_w-\tilde{T}_\infty\right)\beta}\right)$ is bioconvection Rayleigh number, $M\left(=\frac{\sigma B_0^2}{\rho a x^{n-1}}\right)$ is the magnetic parameter, and $\lambda\left(=\frac{\beta^* g(1-C_\infty)(T_w-T_\infty)l}{(m+1)u_e^2}\right)$ is mixed convection parameter, $\mathrm{Pr}\left(=\frac{\nu}{\alpha}\right)$ is the Prandtl number, $Nb\left(=\frac{\tau D_B(C_w-C_\infty)}{\nu}\right)$ is the Brownian motion parameter, $Nt\left(=\frac{\tau D_T(T_w-T_\infty)}{T_\infty\nu}\right)$is the thermophoresis parameter, $Le\left(=\frac{\alpha}{D_B}\right)$ is Lewis number, $Lb\left(=\frac{\nu}{D_m}\right)$ is bioconvection Lewis number and$Pe\left(=\frac{bW_c}{D_m}\right)$is Peclet number

The boundary conditions in dimensionless form are:

$$\left.\begin{array}{c} Me\theta(0)+\mathrm{Pr}f(0), f'(\zeta)|_{\zeta=0}=-1\alpha(1+Ma), \\ \theta'(0)=-A_1(1-\theta(0)), \phi'(0)=-A_2(1-\phi(0)), \\ \chi'(0)=-A_3(1-\chi(0)), at\,\zeta=0 \\ f\to 0, \theta\to 0, \phi\to 0, \chi\to 0\, as\,\zeta\to\infty \end{array}\right\}, \tag{14}$$

Here $Me\left(=\frac{c_p(T_\infty-T_m)}{\lambda+c_s(T_m-T_0)}\right)$ is the melting parameter, $\alpha\left(=\frac{\gamma_T A}{\mu\Omega}\sqrt{\frac{\Omega}{\gamma}}\right)$ is Marangoni number, and $Ma\left(=\frac{\gamma_C B}{\gamma_T A}\right)$ is Marangoni ratio parameter, $A_1\left(=\frac{h_f}{k}\sqrt{\frac{2\nu}{(m+1)U_e}}\right)$ is thermal Biot number, $A_2\left(=\frac{h_g}{D_B}\sqrt{\frac{2\nu}{(m+1)U_e}}\right)$ is concentration Biot number, $A_3\left(=\frac{h_n}{D_m}\sqrt{\frac{2\nu}{(m+1)U_e}}\right)$ is microorganism Biot number.

3. Numerical solution

Eqs. (11)–(14) with boundary conditions (15) are solved numerically by using famous shooting technique by using MATLAB computational software. Since these equations are nonlinear and coupled in nature therefore the exact solution is not possible. The shooting mthod is the most efficient technique to compute the numerical approximation of such type of highly nonlinear problems. This method shows excellent solution accuracy and does not consist of any complicated discretization like other numerical schemes. The accuracy of this numerical is also found to be excellent. In order to simulates the flow problem via this iterative technique, let us assume:

$$\left.\begin{array}{c} f=p_1, f'=p_2, f''=p_3, f'''=p_3', \\ \theta=p_4, \theta'=p_5, \theta''=p_5', \\ \phi=p_6, \phi'=p_7, \phi''=p_7', \\ \chi=p_8, \chi'=p_9, \chi''=p_9' \end{array}\right\}, \tag{15}$$

$$p_3'=\frac{-2p_1p_3+2p_2^2-\beta p_3+(M+\frac{S}{2})p_2-\frac{1}{12}\alpha_2 p_2 p_3^2-\lambda(p_4-Nrp_6-Ncp_8)}{((1+2\beta\zeta)-\frac{\alpha_1}{2}(1+2\beta\zeta)p_3^2)}, \tag{16}$$

$$p_5'=\frac{-\in_1 p_5^2+\frac{1}{\mathrm{Pr}}\beta p_5-p_1p_5+(1+2\beta\zeta)\left[Nbp_5p_7+Ntp_5^2\right]}{\left(\frac{1}{\mathrm{Pr}}(1+2\beta\zeta)+\in_1\right)}, \tag{17}$$

$$p_7'=\frac{-\in_2 p_7^2-\beta p_7-Le\mathrm{Pr}p_1p_7-\frac{Nt}{Nb}\left[(1+2\beta\zeta)p_5'+\beta p_5\right]}{((1+2\beta\zeta)+\in_2)}, \tag{18}$$

$$p_9'=\frac{-2\beta p_9-Lbp_9p_1+Pe\left(p_7'(p_8+\varpi)+p_9p_7\right)}{(1+2\beta\zeta)}, \tag{19}$$

With

$$\left.\begin{array}{c} Mep_4(0)+\mathrm{Pr}p_1(0), p_2(\zeta)|_{\zeta=0}=-1\alpha(1+Ma), \\ p_5(0)=-A_1(1-p_4(0)), p_7(0)=-A_2(1-p_6(0)), \\ p_9(0)=-A_3(1-p_8(0)), at\,\zeta=0 \\ p_1\to 0, p_4\to 0, p_6\to 0, p_8\to 0\, as\,\zeta\to\infty \end{array}\right\}, \tag{20}$$

Table 1 A comparative analysis for obtain numerical results with work of Akbar et al. [51], Taimoor et al. [52] and Bilal et al. [53] when $\alpha_1 = \beta = S = \lambda = \alpha_1 = 0$.

M	Akbar et al. [51]	Taimoor et al. [52]	Bilal et al. [53]	Present results
0.0	1.0000	1.0000	1.0000	1.0000
0.5	−1.11803	−1.11802	−1.11800	−1.11802
1.0	−1.41421	−1.41419	1.41420	−1.41420

4. Solution verification

The solution verification for current modeled flow problem is accessed by comparing the results with work of Akbar et al. [51], Taimoor et al. [52] and Bilal et al. [53] as a limiting case in Table 1. A desirable solution accuracy of obtained solution is noticed with these investigations.

5. Discussion

In this section, we will scrutinize obtained the graphical results of Sutterby nanofluid confined by stretching cylinder with the Melting phenomenon. The influence of various flow parameters is examined with help of various graphs. Fig. 2 shows the behavior of bioconvection Rayleigh number Nc and Marangoni number α on velocity distribution f'. It can be noticed that the increasing values of Marangoni number α causes an intensifying velocity distribution f'. Physically, the Marangoni number presented the comparative analysis for transportation rate due to Marangoni flow and diffusion transportation rate. The higher values of α results a progressive Marangoni flow due to which velocity increases. However, a declining change in velocity is observed with bioconvection Rayleigh number Nc. The physical explanation for such declining behavior is due to presence of buoyancy forces due to bioconvection which retarded the fluid velocity effectively. Fig. 3 is prepared to describe the characteristics of Sutterby nanofluid parameter α_1 and Darcy resistance parameter α_2 on f'. Both parameters effectively reduce the fluid velocity. Physically, the decrement in velocity for higher values of α_2 is due to the fact that Darcy resistance parameter is associated with the permeability of porous medium. Due to higher permeability of porous space, the velocity of nanofluid reduces. Fig. 4 is indicated to show the influence of the Marangoni ratio parameter Ma and buoyancy ratio parameter Nr over the fluid velocity f'. The highest values of Marangoni ratio parameter Ma causes an increasing velocity distribution while an enhancing values of Nr result a decaying f'. Fig. 5 is prepared to examine the influence of melting parameter Me as well as mixed convection parameterλ on f'. It can be noticed that the greater value of melting parameter Me improves the fluid velocity. Moreover, the fluid velocity f' enhanced for mixed convection parameter λ. The higher

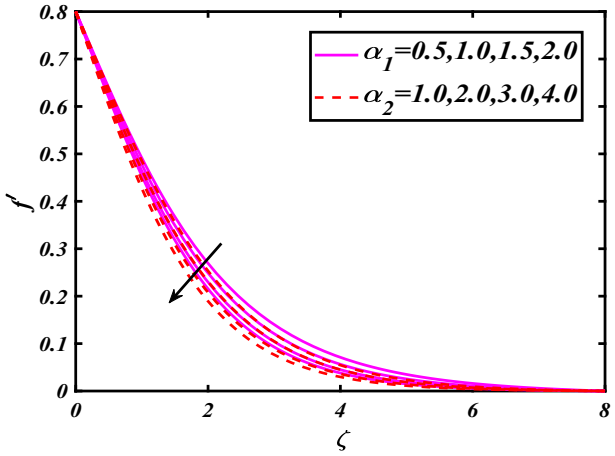

Fig. 3 Impact of α_1 and α_2 on f'.

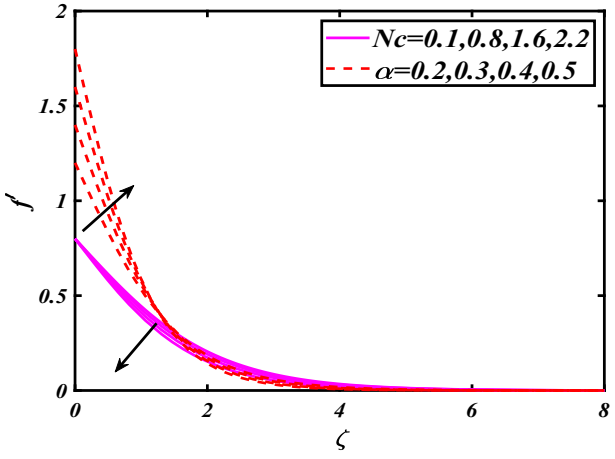

Fig. 2 Impact of Nc and α on f'.

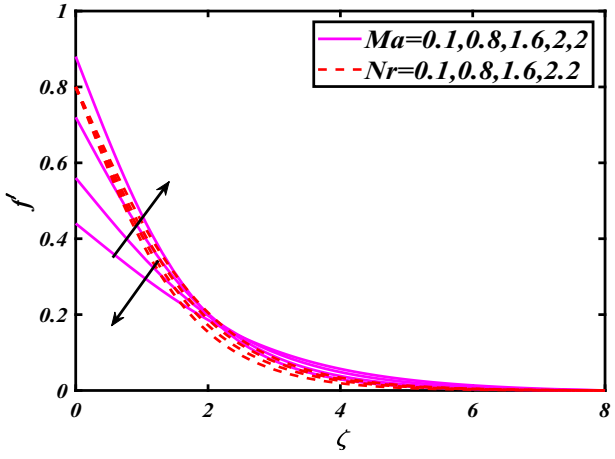

Fig. 4 Impact of Ma and Nr on f'.

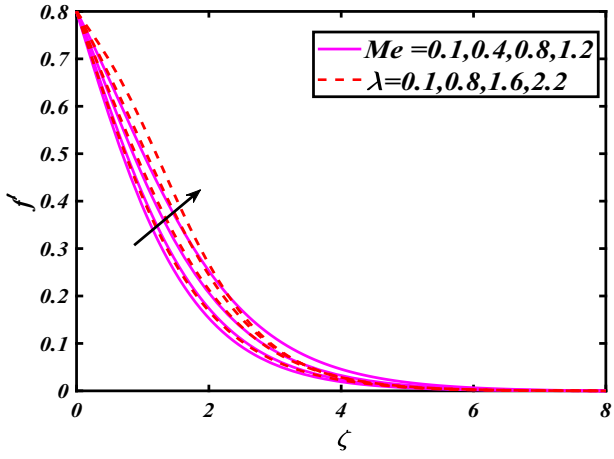

Fig. 5 Impact of Me and λ on f'.

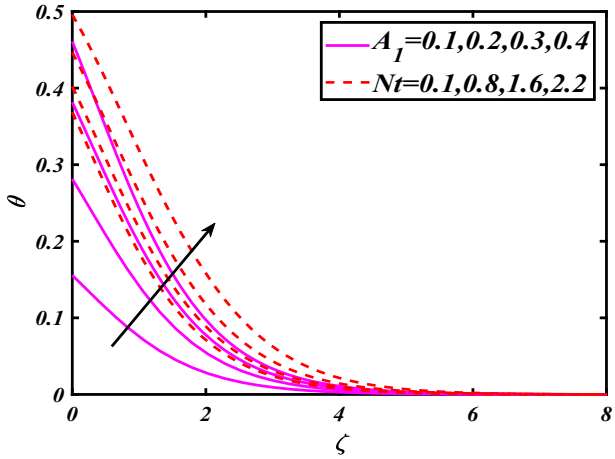

Fig. 7 Impact of A_1 and Nt on θ.

numerical variation of mixed convection parameter attributes larger buoyancy forces which significantly improve the velocity. In order to show the variation of Prandtl number Pr and thermal conductivity parameter $\in_1$ on nanofluid temperature θ, Fig. 6 is plotted**.** It is observed that the enhancing $\in_1$ results a decrement in θ. However, the nanofluid temperature gets decreasing trend with Prandtl numberPr. Physically, the larger values of Pr accomplish less thermal diffusivity which turns down nanofluid temperature. Fig. 7 gives the influence of thermal Biot number A_1 on θ. It can be noticed that the greater value of thermal Biot number A_1 improves the thermal field of species θ. In fact, thermal Biot number is physically related to the coefficient of heat transfer which is responsible to improve the temperature. This figures also incorporates the change in θ due to thermophoresis parameter Nt. The nanofluid temperature θ get enhanced for enlarge values of thermophoresis parameter Nt. The thermophoresis mechanism discloses the movement of nanoparticles towards the surface of lower temperature from heated surface due to temperature. This migrated phenomenon makes variation in nanofluid temperature. Fig. 8 is disclosed to examine the consequence of concentration conductivity parameter $\in_2$ and buoyancy ratio parameter Nr on concentration field of speciesϕ. From this

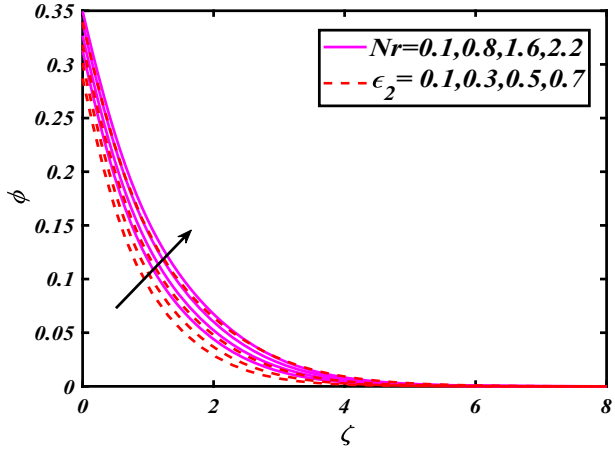

Fig. 8 Impact of Nr and $\in_2$ on ϕ.

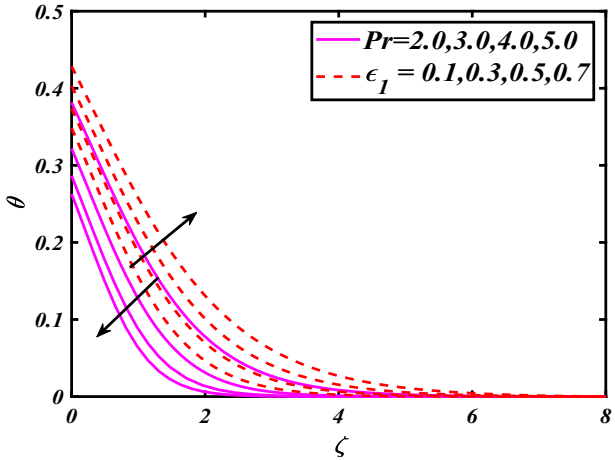

Fig. 6 Impact of Pr and $\in_1$ on θ.

figure, it is observed that the concentration field of species ϕ show increasing change with both $\in_2$ and Nr. Fig. 9 aims to examine the consequence of curvature parameter β and concentration Biot number A_2 on concentration field of species ϕ. It is observed that the concentration field of speciesϕ get increases for curvature parameter β and concentration Biot number A_2. Fig. 10 is designed to securitize the behavior of Brownian motion parameter Nb and thermophoresis parameter Nt on ϕ. The profile of concentration field of species ϕ is enhanced for larger thermophoresis parameter Nt and Brownian motion parameter Nb. Fig. 11 is achieved to display the characteristics of Prandtl number Pr and Lewis number Le against concentration field of speciesϕ. The growing values of Prandtl number and Lewis number Le reduce the concentration field of speciesϕ Physically, the Prandtl number Pr represents the ratio between the thermal conductivity to the thermal diffusivity. Consequently, higher values of Prandtl number lead to reduced thermal diffusivity in addition to weaker values of declined diffusivity appear. The declining variation in concentration associated with larger values of Lewis number is due to the fact that Lewis number attained reverse relation with mass diffusivity. The higher values assign to Lewis number predict the lessened mass diffusivity which control the

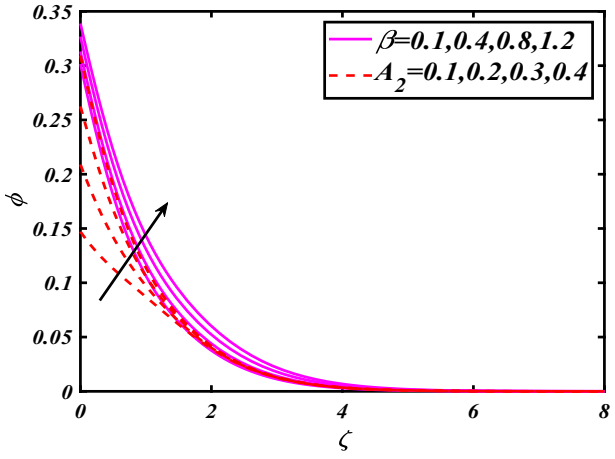

Fig. 9 Impact of β and A_2 on ϕ.

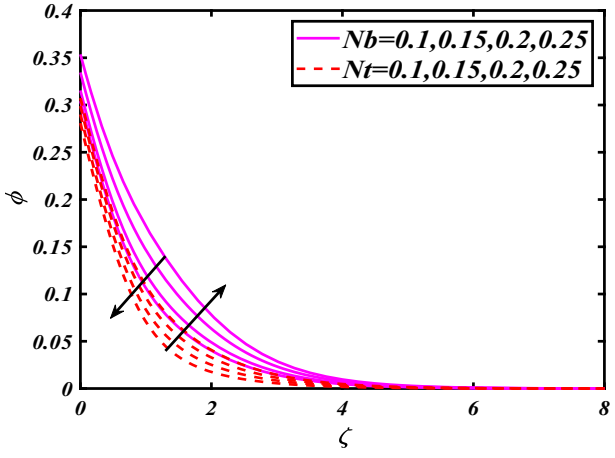

Fig. 10 Impact of Nb and Nt on ϕ.

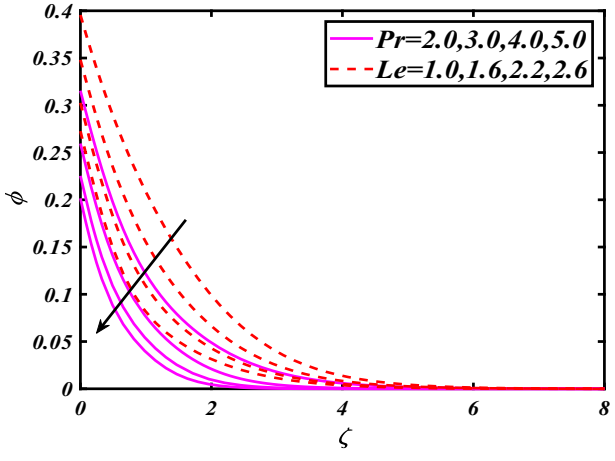

Fig. 11 . Impact of Pr and Le on ϕ.

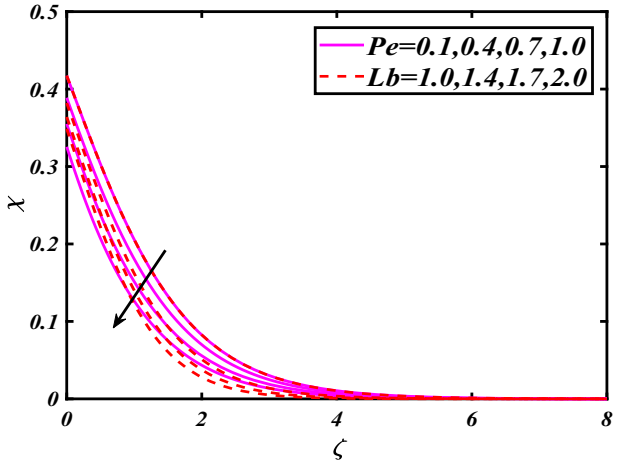

Fig. 12 Impact of Pe and Lb on χ.

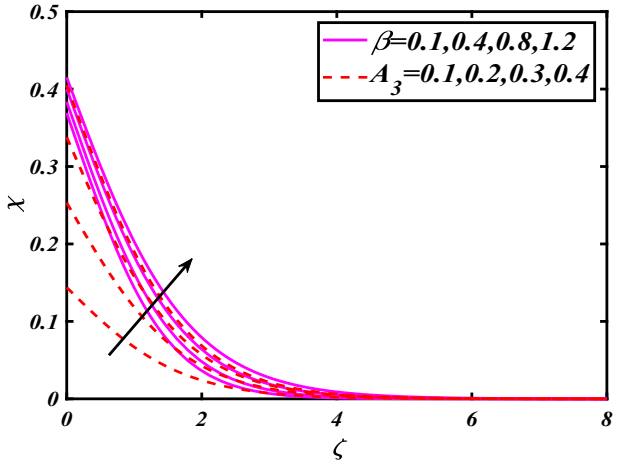

Fig. 13 Impact of β and A_3 on χ.

nanofluid concentration.. Fig. 12 is captured to illustrate the influence of Peclet number Pe and bioconvection Lewis number Lb on microorganism's field χ. It is noted that microorganism's field χ get retarded by enlarging the estimation of Peclet numberPe. The reverse relation of Peclet number with motile diffusivity refeltcs a declining microorganism's profile. From this figure, it can be also noticed larger bioconvection Lewis numberLb decrease the microorganism's field χ. Fig. 13 reveals the impact of microorganism Biot number$A_3$and curvature parameter β via microorganism field χ. Here concentration of microorganism distribution χ is boosted up by growing the amount of microorganism Biot number $A_3$and curvature parameter β.

6. Physical quantities

Table 2 shows the aspect of flow parameters on the local skin friction coefficient. The local skin friction coefficient rises for higher variations Nr,Nc,Me,S and $f''(0)$ declines for larger variationsλ.The numerical estimations of local Nusselt numbers via different flow parameters are shown in Table 3. It can be depicted that the local Nusselt number decreases for

Table 2 Numerical results of $-f''(0)$ versus flow parameters

Flow parameters							*Local skin friction coefficients*
M	λ	Me	S	Nr	Nc	β	$-f''(0)$
0.1	0.2	0.5	0.3	0.1	0.1	0.3	0.1379
0.7							0.1545
0.7							0.1685
0.5	0.1	0.5	0.3	0.1	0.1	0.3	0.1618
	0.3						0.1570
	0.7						0.1474
0.5	0.2	0.1	0.3	0.1	0.1	0.3	0.1525
		0.3					0.1558
		0.7					0.1630
0.5	0.2	0.5	0.1	0.1	0.1	0.3	0.1103
			0.4				0.1764
			0.7				0.2161
0.5	0.2	0.5	0.3	0.2	0.1	0.3	0.1597
				0.4			0.1605
				0.6			0.1601
0.5	0.2	0.5	0.3	0.1	0.2	0.3	0.1600
					0.4		0.1612
					0.6		0.1625
0.5	0.2	0.5	0.3	0.1	0.1	0.1	0.1636
						0.4	0.1800
						0.7	0.1767

Table 3 Numerical results of $-\theta'(0)$ versus flow parameters.

Flow parameters										*Local Nusselt number*
M	λ	Me	Pr	A_1	Nr	Nc	β	Nb	Nt	$-\theta'(0)$
0.1	0.2	0.5	2.0	0.3	0.1	0.1	0.3	0.2	0.3	0.1829
0.7										0.1816
0.7										0.1804
0.5	0.1	0.5	2.0	0.3	0.1	0.1	0.3	0.2	0.3	0.1810
	0.3									0.1814
	0.7									0.1820
0.5	0.2	0.1	2.0	0.3	0.1	0.1	0.3	0.2	0.3	0.1771
		0.3								0.1791
		0.7								0.1832
0.5	0.2	0.5	3.0	0.3	0.1	0.1	0.3	0.2	0.3	0.1949
			4.0							0.2034
			5.0							0.2092
0.5	0.2	0.5	2.0	0.1	0.1	0.1	0.3	0.2	0.3	0.0821
				0.4						0.2133
				0.7						0.2761
0.5	0.2	0.5	2.0	0.3	0.2	0.1	0.3	0.2	0.3	0.1812
					0.4					0.1811
					0.6					0.1820
0.5	0.2	0.5	2.0	0.3	0.1	0.2	0.3	0.2	0.3	0.1811
						0.4				0.1809
						0.6				0.1808
0.5	0.2	0.5	2.0	0.3	0.1	0.1	0.1	0.2	0.3	0.1836
							0.4			0.1800
							0.7			0.1767
0.5	0.2	0.5	2.0	0.4	0.1	0.1	0.3	0.1	0.3	0.1831
								0.3		0.1793
								0.5		0.1754
0.5	0.2	0.5	2.0	0.4	0.1	0.1	0.3	0.2	0.1	0.1851
									0.4	0.1792
									0.7	0.1728

Table 4 Numerical results of $\phi'(0)$ versus flow parameters

Flow parameters											Local Sherwood number
M	λ	Me	Pr	Le	Nr	Nc	β	A_2	Nb	Nt	$-\phi'(0)$
0.1	0.2	0.5	2.0	2.0	0.1	0.1	0.3	0.4	0.2	0.3	0.2750
0.7											0.2742
0.7											0.2736
0.5	0.1	0.5	2.0	2.0	0.1	0.1	0.3	0.4	0.2	0.3	0.2739
	0.3										0.2741
	0.7										0.2745
0.5	0.2	0.1	2.0	2.0	0.1	0.1	0.3	0.4	0.2	0.3	0.2703
		0.3									0.2721
		0.7									0.2759
0.5	0.2	0.5	3.0	2.0	0.1	0.1	0.3	0.4	0.2	0.3	0.2924
			4.0								0.3046
			5.0								0.3134
0.5	0.2	0.5	2.0	3.0	0.1	0.1	0.3	0.4	0.2	0.3	0.2975
				4.0							0.3119
				5.0							0.3219
0.5	0.2	0.5	2.0	2.0	0.2	0.1	0.3	0.4	0.2	0.3	0.2740
					0.4						0.2738
					0.6						0.2736
0.5	0.2	0.5	2.0	2.0	0.1	0.2	0.3	0.4	0.2	0.3	0.2740
						0.4					0.2737
						0.6					0.2734
0.5	0.2	0.5	2.0	2.0	0.1	0.1	0.1	0.4	0.2	0.3	0.2776
							0.4				0.2723
							0.7				0.2675
0.5	0.2	0.5	2.0	2.0	0.1	0.1	0.3	0.1	0.2	0.3	0.0843
								0.3			0.2192
								0.7			0.4037
0.5	0.2	0.5	2.0	2.0	0.1	0.1	0.3	0.4	0.1	0.3	0.2480
									0.3		0.2826
									0.5		0.2894
0.5	0.2	0.5	2.0	2.0	0.1	0.1	0.3	0.4	0.2	0.1	0.2895
										0.4	0.2672
										0.7	0.2505

larger estimations M,Nt,Nt while it booms for the remaining parameter. Furthermore, the greaterλ and Pradvance the heat transfer. Table 4 scrutinizes the variation in local Sherwood number $-\phi'(0)$against different parameters. From this study, it can be investigated that the local Sherwood number $-\phi'(0)$ is rising M,Nr,β. It is also observed that Me and A_2 influences augment the local Sherwood number$-\phi'(0)$. From Table 5 the numerical estimation of local microorganism's density number scrutinized that it intensifies for Lb,Pe, while it diminishes with β. Also, variations of microorganism density number are boosted up with A_3.

7. Concluding observations

The two-dimensional flow of Sutterby nanofluids over a stretching cylinder is scrutinized in the presence of bioconvection and swimming microorganisms. The effect of bioconvectional flow analyzed with thermal conductivity. The Marangoni and solutal boundaries with melting phenomenon are considered as a novelty. The shooting algorithm is imposed in order to achieve the numerical computations. Key observations of investigations are as follows:

- Velocity profile enhanced by amplification in the values of mixed convection parameter and Marangoni ratio parameter while opposite nature is noticed for the buoyancy ratio parameter.
- Change in Sutterby nanofluid parameter and Darcy resistance parameter effectively controls the motion of fluid particles.
- The thermal of species is boom up by increasing the amount of thermal conductivity and thermal Biot number.
- The concentration of species boomed for higher concentration Biot number and buoyancy ratio parameter.
- An arising change in concentration is noticed with curvature parameter and concentration conductivity parameter.
- Microorganism's field is decreased for distinguished magnitudes of Peclet number and bioconvection Lewis number.
- The microorganism profile get enhanced with maximum variation of Biot number and bioconvection Rayleigh number.

Table 5 Numerical results solutions $-\chi'(0)$versus flow parameters.

Flow parameters									Local microorganism number
M	λ	Me	Lb	Pe	Nr	Nc	β	A_3	$-\chi'(0)$
0.1	0.2	0.5	1.0	0.1	0.1	0.1	0.3	0.4	0.2295
0.7									0.2276
0.7									0.2261
0.5	0.1	0.5	1.0	0.1	0.1	0.1	0.3	0.4	0.2269
	0.3								0.2273
	0.7								0.2282
0.5	0.2	0.1	1.0	0.1	0.1	0.1	0.3	0.4	0.2221
		0.3							0.2246
		0.7							0.2296
0.5	0.2	0.5	2.0	0.1	0.1	0.1	0.3	0.4	0.2661
			4.0						0.2997
			6.0						0.3165
0.5	0.2	0.5	1.0	0.2	0.1	0.1	0.3	0.4	0.2315
				0.4					0.2399
				0.6					0.2477
0.5	0.2	0.5	1.0	0.1	0.2	0.1	0.3	0.4	0.2271
					0.4				0.2270
					0.6				0.2268
0.5	0.2	0.5	1.0	0.1	0.1	0.2	0.3	0.4	0.2270
						0.4			0.2269
						0.6			0.2261
0.5	0.2	0.5	1.0	0.1	0.1	0.1	0.1	0.4	0.2227
							0.4		0.2292
							0.7		0.2349
0.5	0.2	0.5	1.0	0.1	0.1	0.1	0.3	0.1	0.0842
								0.3	0.1911
								0.7	0.2997

References

[1] S.U.S. Choi (Ed.), Enhancing Thermal Conductivity of Fluids with Nanoparticles, vol. 231, ASME Publications-Fed, 1995, pp. 99–106.

[2] J. Buongiorno, Convective transport in nanofluids, J. Heat Transf. 28 (2006) 240–250.

[3] S. Islam, A. Khan, W. Deebani, E. Bonyah, N.A. Alreshidi, Z. Shah, Influences of Hall current and radiation on MHD micropolar non-Newtonian hybrid nanofluid flow between two surfaces, AIP Adv. 10 (5) (2020) 055015.

[4] S.M. Alempour, A.A.A. Arani, M.M. Najafizadeh, Numerical investigation of nanofluid flow characteristics and heat transfer inside a twisted tube with elliptic cross section, J. Therm. Anal. Calorim. 140 (2020) 1237–1257.

[5] M. Ghalambaz, T. Groşan, I. Pop, Mixed convection boundary layer flow and heat transfer over a vertical plate embedded in a porous medium filled with a suspension of nano-encapsulated phase change materials, J. Mol. Liq. 293 (1) (2019) 111432.

[6] P. Naga Santoshi, G.V. Ramana Reddy, P. Padma, Numerical scrutinization of three dimensional Casson-Carreau nano fluid flow, J. Appl. Computat. Mech. 6 (3) (2020) 531–542.

[7] Y. Wang, K. Deng, J.M. Wu, G. Su, S. Qiu, A mechanism of heat transfer enhancement or deterioration of nanofluid flow boiling heat transfer, Int. J. Heat Mass Transf. 158 (2020) 119985.

[8] Nilankush Acharya, Kalidas Das, Prabir Kumar Kundu, Framing the features of MHD boundary layer flow past an unsteady stretching cylinder in presence of non-uniform heat source, J. Mol. Liquids, Volume 225, January 2017, Pages 418-425.

[9] Nilankush Acharya, Kalidas Das, Prabir Kumar Kundu, Framing the effects of solar radiation on magneto-hydrodynamics bioconvection nanofluid flow in presence of gyrotactic microorganisms, J. Mol. Liquids 222 (2016) 28–37.

[10] Kalidas Das, Nilankush Acharya and Prabir Kumar Kundu , Influence of Variable Fluid Properties on Nanofluid Flow over a Wedge with Surface Slip, Arabian Journal for Science and Engineering volume 43, pages2119–2131(2018).

[11] Nilankush Acharya, Kalidas Das, Prabir Kumar Kundu, Outlining the impact of second-order slip and multiple convective condition on nanofluid flow: a new statistical layout, Can. J. Phys. 96 (1) (2018) 104-111.

[12] Nilankush Acharya, Spectral quasi linearization simulation of radiative nanofluidic transport over a bended surface considering the effects of multiple convective conditions, Eur. J. Mech. B. Fluids 84 (2020) 139–154.

[13] I. Tlili, N. Shahmir, M. Ramzan, S. Kadry, J.Y. Kim, Y. Nam, D. Lu, A novel model to analyze Darcy Forchheimer nanofluid flow in a permeable medium with Entropy generation analysis, J. Taibah Univ. Sci. 14 (1) (2020) 916–930.

[14] M. Amjad, I. Zehra, S. Nadeem, N. Abbas, Thermal analysis of Casson micropolar nanofluid flow over a permeable curved stretching surface under the stagnation region, J. Therm. Anal. Calorim. (2020), https://doi.org/10.1007/s10973-020-10127-w.

[15] M. Atashafrooz, Influence of radiative heat transfer on the thermal characteristics of nanofluid flow over an inclined step in the presence of an axial magnetic field, J. Therm. Anal. Calorim. 139 (5) (2020) 3345–3360.

[16] N.A. Mir, M. Farooq, M. Rizwan, F. Ahmad, S. Ahmad, B. Ahmad, Analysis of thermally stratified flow of Sutterby nanofluid with zero mass flux condition, J. Mater. Res. Technol. 9 (2) (2020) 1631–1639.

[17] M. Nawaz, Role of hybrid nanoparticles in thermal performance of Sutterby fluid, the ethylene glycol, Physica A 1 (537) (2020) 122447.

[18] S. Bilal, M. Sohail, R. Naz, M.Y. Malik, Dynamical and optimal procedure to analyze the exhibition of physical attributes imparted by Sutterby magneto-nanofluid in Darcy medium yielded by axially stretched cylinder, Can. J. Phys. 98 (1) (2020) 1.
[19] Mohsan Hassan, Essam R El-Zahar, Sami Ullah Khan, Mohammad Rahimi-Gorji, Ashfaq Ahmad, Boundary layer flow pattern of heat and mass for homogenous shear thinning hybrid-nanofluid: An experimental data base modeling, Numerical Methods for Partial Differential Equations, Volume 37, Issue2, March 2021, pp. 1234-1249.
[20] Kh. Hosseinzadeh, M.A. Erfani Moghaddam, A. Asadi, A.R. Mogharrebi, B. Jafari, M.R. Hasani, D.D. Ganji, Effect of two different fins (longitudinal-tree like) and hybrid nano-particles (MoS_2-TiO_2) on solidification process in triplex latent heat thermal energy storage system, Alex. Eng. J. 60 (1) (2021) 1967–1979.
[21] Kh. Hosseinzadeh, So. Roghani, A. R. Mogharrebi, A. Asadi & D. D. Ganji, Optimization of hybrid nanoparticles with mixture fluid flow in an octagonal porous medium by effect of radiation and magnetic field, Journal of Thermal Analysis and Calorimetry volume, 143, pp. 1413–1424(2021).
[22] B. Mahanthesh, S.A. Shehzad, T. Ambreen, S.U. Khan, Significance of Joule heating and viscous heating on heat transport of MoS_2–Ag hybrid nanofluid past an isothermal wedge, J. Therm. Anal. Calorim. 143 (2021) 1221–1229.
[23] J.R. Platt, Bioconvection patterns in cultures of free-swimming organisms, Science 133 (80) (1961) 1766–1767.
[24] M.S. Plesset, H. Wine, Bioconvection patterns in swimming microorganism cultures as an example of Rayleigh-Taylor instability, Nature 248 (1974) 441–443.
[25] A.V. Kuznetsov, The onset of nanofuid bioconvection in a suspension containing both nanoparticles and gyrotactic microorganisms, Int. Commun. Heat Mass Transf. 37 (10) (2010) 1421–1425.
[26] Y.M. Chu, S. Aziz, M.I. Khan, S.U. Khan, M. Nazeer, I. Ahmad, I. Tlili, Nonlinear radiative bioconvection flow of Maxwell nanofluid configured by bidirectional oscillatory moving surface with heat generation phenomenon, Phys. Scr. 95 (10) (2020) 105007.
[27] S. Islam, M. Jawad, A. Saeed, Z. Shah, M. Zubair, A. Khan, H. Alrabaiah, MHD Darcy-Forchheimer flow due to gyrotactic microorganisms of Casson nanoparticles over a stretched surface with convective boundary conditions, Phys. Scr. 96 (1) (2020) 015206.
[28] N.S. Khan, Q. Shah, A. Sohail, Dynamics with Cattaneo-Christov heat and mass flux theory of bioconvection Oldroyd-B nanofluid, Adv. Mech. Eng. 12 (8) (2020) 1–20.
[29] H. Waqas, S.U. Khan, I. Tlili, M. Awais, M.S. Shadloo, Significance of bioconvective and thermally dissipation flow of viscoelastic nanoparticles with activation energy features: novel biofuels significance, Symmetry 12 (2) (2020) 214.
[30] M. Ferdows, A. Hossan, M.Z.I. Bangalee, S. Sun, F. Alzahrani, Stability theory of nano-fluid over an exponentially stretching cylindrical surface containing microorganisms, Sci. Rep. 10 (1) (2020) 1–18.
[31] T. Sajid, M. Sagheer, S. Hussain, F. Shahzad, Impact of double-diffusive convection and motile gyrotactic microorganisms on magnetohydrodynamics bioconvection tangent hyperbolic nanofluid, Open Physics 18 (1) (2020) 74–88.
[32] H. Waqas, S.U. Khan, S.A. Shehzad, M. Imran, Significance of the nonlinear radiative flow of micropolar nanoparticles over porous surface with a gyrotactic microorganism, activation energy, and Nield's condition, Heat Transfer—Asian Research 48 (7) (2019) 3230–3256.
[33] Y. Li, H. Waqas, M. Imran, U. Farooq, F. Mallawi, I. Tlili, A numerical exploration of modified second-grade nanofluid with motile microorganisms, thermal radiation, and Wu's slip, Symmetry 12 (3) (2020) 393.
[34] M.I. Khan, Transportation of hybrid nanoparticles in forced convective Darcy-Forchheimer flow by a rotating disk, Int. Commun. Heat Mass Transfer 122 (2021) 105177.
[35] N.I. Nima, M. Ferdows, M.M. Ardekani, Effects of Cross diffusion and radiation on magneto mixed convective stagnation flow from a vertical surface in porous media with Gyrotactic Microorganisms: similarity and numerical analysis, Spec. Top. Rev. Porous Media: Int. J. 11 (3) (2020) 203–219.
[36] A. Aly, MHD Boundary layer flow of a power-law nanofluid containing gyrotactic microorganisms over an exponentially stretching surface, Comput. Mater. Continua 62 (2) (2020) 525–549.
[37] S. Rana, R. Mehmood, S. Nadeem, Bioconvection through interaction of Lorentz force and gyrotactic microorganisms in transverse transportation of rheological fluid, J. Therm. Anal. Calorimet., https://doi.org/10.1007/s10973-020-09830-5.
[38] T. Sajid, S. Tanveer, M. Munsab, Z. Sabir, Impact of oxytactic microorganisms and variable species diffusivity on blood-gold Reiner-Philippoff nanofluid, Appl. Nanoscience (2020), https://doi.org/10.1007/s13204-020-01581-x.
[39] Haq, F., Khan, M. I., Khan, S. A., & Hayat, T. (2020). Investigation of suspended nanoliquid flow of Eyring–Powell fluid with gyrotactic microorganisms and density number. Advances in Mechanical Engineering, 12(9) 1–10.Shahid, A., Huang, H., Bhatti, M. M., Zhang, L., & Ellahi, R. (2020). Numerical investigation on the swimming of gyrotactic microorganisms in nanofluids through porous medium over a stretched surface. Mathematics, 8(3), 380.
[40] Mogharrebi, A. R., D. Ganji, A.R., Hosseinzadeh, K., Roghani, S., Asadi, A. and Fazlollahtabar, A., Investigation of magnetohydrodynamic nanofluid flow contain motile oxytactic microorganisms over rotating cone, International Journal of Numerical Methods for Heat & Fluid Flow,(2021), https://doi.org/10.1108/HFF-08-2020-0493.
[41] Kh. Hosseinzadeh, So. Roghani, A.R. Mogharrebi, A. Asadi, M. Waqas, D.D. Ganji, Investigation of cross-fluid flow containing motile gyrotactic microorganisms and nanoparticles over a three-dimensional cylinder, Alex. Eng. J. 59 (5) (2020) 3297–3307.
[42] J.L. Sutterby, Laminar converging flow of dilute polymer solutions in conical sections: part I. viscosity data, new viscosity model, tube flow solution, AICHE J. 12 (1966) 63–68.
[43] N.S. Akbar, Biomathematical study of Sutterby fluid model for blood flow in stenosed arteries, Int. J. Biomath. 8 (6) (2015). Article 1550075.
[44] T. Hayat, S. Ayub, A. Alsaedi, A. Tanveer, B. Ahmad, Numerical simulation for peristaltic activity of Sutterby fluid with modified Darcy's law, Results Phys 7 (2017) 762–768.
[45] Z. Abbas, M.S. Shabbir, N. Ali, Numerical study of magnetohydrodynamic pulsatile flow of Sutterby fluid through an inclined overlapping arterial stenosis in the presence of periodic body acceleration, Results Phys 9 (2018) 753–762.
[46] T. Hayat, M. Ijaz Khan, M. Farooq, A. Alsaedi, T. Yasmeen, Impact of Marangoni convection in the flow of carbon–water nanofluid with thermal radiation, Int. J. Heat Mass Transf. 106 (2017) 810–815.
[47] Y.J. Zhuang, Q.Y. Zhu, Numerical study on combined buoyancy–Marangoni convection heat and mass transfer of power-law nanofluids in a cubic cavity filled with a heterogeneous porous medium, Int. J. Heat Mass Transf. 71 (2018) 39–54.
[48] T.S. Wang, W.Y. Shi, Influence of substrate temperature on Marangoni convection instabilities in a sessile droplet evaporating at constant contact line mode, Int. J. Heat Mass Transf. 131 (2019) 1270–1278.
[49] Mohammad Ghalambaz, Seyed Mohsen Hashem Zadeh, S. A. M. Mehryan, Ioan Pop, Dongsheng Wen, Analysis of melting behavior of PCMs in a cavity subject to a non-uniform magnetic

field using a moving grid technique, Applied Mathematical Modelling, Volume 77, Part 2, January 2020, Pages 1936-1953.
[50] Mohammad Ghalambaz, Jun Zhang, Conjugate solid-liquid phase change heat transfer in heatsink filled with phase change material-metal foam, Int. J. Heat Mass Transf. 146 (2020) 118832.
[51] N.S. Akbar, A. Ebai, Z.H. Khan, Numerical analysis of magneticeld effects on Eyring. Powell fluid flow towards a stretching sheet, J. Magn. Magn. Mater. 382 (2015) 355.
[52] M.Y. Malik, T. Salahuddin, A. Hussain, S. Bilal, MHD flow of tangent hyperbolic fluid over a stretching cylinder: using Keller box method, J. Magn. Magn. Mater. 395 (2015) 271.
[53] S. Bilal, M. Sohail, R. Naz, M.Y. Malik, Dynamical and optimal procedure to analyze the exhibition of physical attributes imparted by Sutterby magneto-nanofluid in Darcy medium yielded by axially stretched cylinder, Can. J. Phys. 98 (1) (2020).